

Multiresonator quantum memory with atomic ensembles

S.A. Moiseev*

*Kazan Quantum Center, Kazan National Research Technical University
n.a. A.N. Tupolev-KAI, 10 K. Marx St., 420111, Kazan, Russia*

(Dated: 11 июля 2025 г.)

The theory of multiresonator quantum memory with atomic ensembles has been developed. Using the obtained analytical solutions, the basic physical properties of such memory are analyzed and optimal conditions for its implementation are determined. Advantages of this quantum memory and its experimental implementation in integrated optical schemes are discussed.

I. INTRODUCTION

The use of atomic ensembles [1–7] is one of the most promising approaches in creating multi-qubit quantum memory (QM) [8, 9]. In the last decade, the optical QM schemes have been actively developed, in which atomic ensembles are placed in optical resonators [10–16]. The interest in developing resonator QM schemes is due to a number of interesting properties and advantages. The use of resonators enhances the interaction of photons with atoms, which makes it possible to reduce the optical density of the resonant transition of the atomic ensemble, thereby significantly facilitating the conditions for achieving highly efficient quantum memory. The latter, in turn, facilitates the achievement of a longer coherence time of resonant transitions due to the significant suppression of interparticle interactions. In addition, it is possible to reduce the size of the QM cell in the same way. Resonators can also be directly integrated into waveguide circuits, which opens up the possibility of creating compact quantum devices containing QM along with various processors.

The greatest advantages of resonator QM are demonstrated when using high-quality resonators, in which it is possible to maximize the coupling constant of the photon with atoms. At the same time, an increase in the Q-factor of the resonator narrows the operating range of the QM. For this reason, the placement of the atomic ensemble in a resonator connected to an external waveguide with constant coupling κ , does not provide the maximum spectral width of such an effective QM of more than $\kappa/3$ [17]. An increase in the working spectral width is possible through the use of so-called white resonators [18] and by using several resonators with different frequencies connected to the waveguide directly [19], or through a common resonator [20]. Multiresonator schemes themselves have already proven to be promising for microwave QM [21], and have made it possible to achieve a fairly high efficiency of $\sim 60\%$ when storing Gaussian single-photon wave packets [22, 23].

The multiresonator QM is becoming an interesting physical system, since in it the quantum state of the signal pulse can be preserved for a long time in a system

of spatially remote resonators. The study of the quantum properties of such a physical system is made possible by using individual field control in each of the resonators. In addition to the fundamental interest in similar quantum states [24], the availability of individual control of each resonator opens up new possibilities in the operation of such QM and its use in quantum processing. An important step in improving the capabilities of the multiresonator QM is the development of methods for using atomic ensembles in it. This will increase both its lifetime and the number of stored photonic qubits.

In the first work devoted to the development of such schemes [25], it was shown that it is possible to achieve high efficiency by using atomic ensembles with fewer atoms compared to the generally accepted impedance matched single-resonator scheme [17, 26]. The use of several atomic ensembles in a multiresonator circuit complicates the analytical analysis, therefore, these results were obtained numerically and many general patterns and conditions for the effective implementation of the storage and retrieval of signal light pulses remained unexplored. The improvement of integrated technologies in the manufacture of multiresonator optical circuits [27] raises interest in the development of QM based on atomic ensembles in a system of ring resonators combined in a compact circuit [28]. In this recent work, the authors studied in more detail the operating modes of such QM using numerical methods and showed its practical advantages in working with broadband light fields. However, the basic physical properties of the mechanism of functioning of this QM have still remained unexplored, which is why the conditions for the implementation of high efficiency and the optimal parameters for its implementation remain unknown.

The present work is devoted to the construction of the theory of QM on atomic ensembles in a multiresonator scheme and obtaining analytical results which provide detailed information on the physical processes and mechanism of functioning of such QM, as well as analyzing the influence of its basic parameters on the main properties in storing signal light fields. The aim of this theory is also to develop a working model of the studied QM, which could be experimentally implemented. The developed theory analytically explains the results obtained numerically in previous works [28, 29]. The obtained results also make it possible to

* s.a.moiseev@kazanqc.org

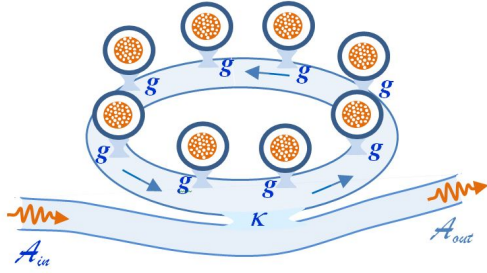


Рис. 1. Spatial scheme of multiresonator quantum memory with atomic ensembles: κ and g are the coupling constants of a common resonator with a waveguide and with mini-resonators; A_{in} and A_{out} are the input and output fields; 8 rings with smaller dark rings containing white dots represent mini-resonators with atomic ensembles located in them; j -th atom interacts with the mode of m -th mini-resonator with a coupling constant $f_{j,m}$.

determine the influence of the physical parameters of the system of atoms and resonators, at which the studied QM can demonstrate the best operation and maximum efficiency.

II. PHYSICAL MODEL AND BASIC EQUATIONS

Similar to works [25, 28], we consider a multiresonator QM scheme, including a system of mini-resonators, which contain atomic ensembles where all mini-resonators are connected to an external waveguide through a common resonator. Note that the use of a common resonator facilitates the operation of such a QM using the controlled connection of this resonator with the external waveguide when the information recorded in the QM continues to be stored in the system of mini-resonators. The developed QM is based on the generalization of the principles of spin (photon) echo [30, 31] into quantum systems that provide reversible dynamics not only of resonant spin (atomic) ensembles, but also of electromagnetic (light) fields interacting with them, as it was first demonstrated in the QM protocol [32] for CRIB protocol and later its implementation was developed in a resonator under the impedance matching condition [17] and similarly for the AFC protocol [26].

The schematic diagram of the QM under study is shown in Fig.1. Identical atomic ensembles are placed in several mini-resonators. The frequencies of the mini-resonators form a periodic frequency comb $\omega_m = \omega_c + m\Delta$ ($m = 0, \pm 1, \pm 2, \dots, M$ is a number of mini-resonators) similar to AFC protocol of QM [33] and realized microwave multiresonator QM [22]. With a large number of mini-resonators, we have equality with high accuracy $\delta_{in} \cong M\Delta$. However, with a small number of mini-resonators M , the determination of the spectral width of the QM requires special consideration, since

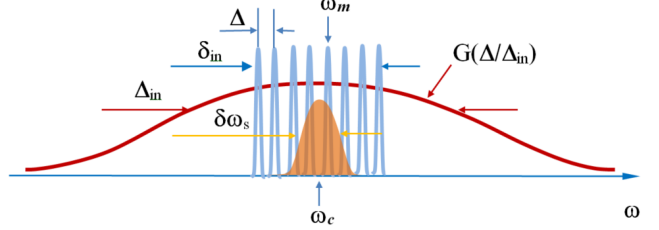


Рис. 2. Spectrum of inhomogeneously broadened atomic ensemble (line shape $G(\Delta/\Delta_{in})$), mini-resonators and signal pulse; Δ is spectral distance between nearest frequencies of mini-resonators, Δ_{in} , δ_{in} and $\delta\omega_s$ are the spectral widths of atomic ensembles, mini-resonators and signal pulse.

it will be necessary to additionally take into account the spectral neighborhoods near the extreme left and right frequencies. In order not to go into the technical details, we will keep the original definition $\delta_{in} \equiv M\Delta$. The central frequency of the optical transition of atoms is tuned to the center of the frequency combs ω_c of the mini-resonators. At the same time, we assume that the line of optical transition of atoms is inhomogeneously broadened, the spectral width of which (Δ_{in}) is much wider than the spectral width (δ_{in}) of the mini-resonator system ($\Delta_{in} \gg \delta_{in}$). Thus, the identical ensembles of atoms are placed in all the mini-resonators having different frequencies, located inside an inhomogeneous broadening of the atomic transition line. Fig. 2 shows the arrangement of the mini-resonator lines, the inhomogeneously broadened line of atomic transition, and the spectrum of the signal pulse.

Before storage of the input signal pulse, the atoms and resonator modes are prepared in the ground state. The behavior of the system under consideration is described by an equations using the input-output approach of quantum optics [34]:

$$\frac{\partial}{\partial t} \hat{a} = -\left(\frac{\kappa}{2} + \gamma_c\right) \hat{a} - i \sum_m^M g_m \hat{b}_m + \sqrt{\kappa} \hat{A}_{in} + \hat{F}_c(t), \quad (1)$$

$$\begin{aligned} \frac{\partial \hat{b}_m}{\partial t} = & - (i\Delta_m + \gamma_b) \hat{b}_m \\ & - ig_m^* \hat{a} - i \sum_j f_{j,m} \hat{S}_{j,m} + \hat{F}_m(t), \end{aligned} \quad (2)$$

$$\frac{\partial \hat{S}_{j,m}}{\partial t} = - (i\delta_{j,m} + \gamma_a) \hat{S}_{j,m} - i f_{j,m}^* \hat{b}_m + \hat{F}_{j,m}(t), \quad (3)$$

where \hat{A}_{in} , \hat{a} , \hat{b}_m are the amplitudes of the input signal, common and m -th mini-resonator modes, $\hat{S}_{j,m}$ is a coherence at the transition $|1\rangle \leftrightarrow |2\rangle$ of j -th atom situated in m -th cavity; $\hat{F}_c(t)$, $\hat{F}_m(t)$, $\hat{F}_{j,m}(t)$ are the Langevin forces related to the decay constants γ_c , γ_b , γ_a ; g_m and f_{jm} are the coupling constants of the common cavity with m -th cavity and j -th atom with m -th cavity

mode.

A. General dynamics and impedance matching conditions

Taking into account the linear nature of the Eqs.(1)-(3) and focusing primarily on finding the condition for achieving maximum QM efficiency with a weak influence of decoherence, we will limit our consideration to the average values of atomic and field operators ($S_{j,m} = \langle \hat{S}_{j,m} \rangle$, $b_m = \langle \hat{b}_m \rangle$, $a = \langle \hat{a} \rangle$, $a_{in} = \langle \hat{a}_{in} \rangle$) and omit the Langevin forces further. In the process of solving the system of Eqs. (1)-(3), we will specify the parameters of the model under study, the constant interactions used in it, the frequencies of the mini-resonators, and the nature of the inhomogeneous broadening of the atomic transition. To find a solution to the system of equations, we begin by writing down a formal solution for the coherence of j -th atom in m -th mini-resonator $\hat{S}_{j,m}(t)$ and substituting it in Eq. (2):

$$S_{j,m}(t) = -i f_{j,m}^* \int_{-\infty}^t dt' b_m(t') \cdot \exp\{-(i\delta_{j,m} + \gamma_a)(t - t')\}, \quad (4)$$

$$\frac{\partial b_m}{\partial t} = - (i\Delta_m + \gamma_b) \hat{b}_m - i g_m^* \hat{a} - N_m f_m^2 \int_{-\infty}^t dt' b_m(t') \exp\{-(\Delta_{in} + \gamma_a)(t - t')\}, \quad (5)$$

where, when calculating the total response of N_m atoms in m -th resonator, we switched to a continuous distribution of atomic frequencies and took into account a large inhomogeneous broadening of the atomic transition Δ_{in} , at which we can take it in the form of a Lorentzian distribution by transferring from discrete (δ_{jm}) to continuous frequency variables (ω_m):

$$\sum_j |f_{j,m}|^2 S_{j,m}(t) \rightarrow N_m f_m^2 \int d\omega_m \frac{\Delta_{in}}{\pi(\Delta_{in}^2 + \omega_m^2)} S(\omega_m, t). \quad (6)$$

Using the Fourier transform for the mode amplitudes $b_m(t) = \frac{1}{\sqrt{2\pi}} \int d\omega \tilde{b}_m(\omega) e^{-i\omega t}$ and $a(t) = \frac{1}{\sqrt{2\pi}} \int d\omega \tilde{a}(\omega) e^{-i\omega t}$, we get the solution of Eq.(5):

$$\tilde{b}_m(\omega) = -i g_m^* \frac{1}{\gamma_b + \frac{N_m f_m^2}{\Delta_{in,a} - i\omega} + i(\Delta_m - \omega)} \tilde{a}(\omega) = -i g_m^* M_m(\Delta_m, \omega) \tilde{a}(\omega) \quad (7)$$

where $\Delta_{in,a} = \Delta_{in} + \gamma_a$.

Assuming the parameters of the atomic ensembles in all mini-resonators to be the same ($N_m = N$, $f_m = f$) and the coupling constants of the mini-resonators with the common resonator to be the same ($g_m = g$) and substituting them into the equation for the field mode in the common resonator, we obtain a solution for the Fourier image of the mode:

$$\tilde{a}(\omega) = T_{cw}(\omega) \tilde{A}_{in}(\omega) = \frac{\sqrt{\kappa} \tilde{A}_{in}(\omega)}{\left(\frac{1}{2}\kappa + \gamma_c - i\omega + g^2 \int d\Delta_m G_r(\frac{\Delta_m}{\delta_{in}}) M_m(\Delta_m, \omega) \right)}, \quad (8)$$

where $G_r(\frac{\Delta_m}{\delta_{in}})$ is a form factor describing the frequency distribution of mini-resonators

$$G_r(\frac{\omega'}{\delta_{in}}) = \text{Lim}_{\gamma_b \rightarrow 0} \sum_{m=1}^M \frac{|g_m/g|^2 \gamma_b}{\pi(\gamma_b^2 + (\omega' - \omega_m)^2)}, \quad (9)$$

where $\omega_m = \omega_c + m\Delta$, $m = 0, \pm 1, \pm 2, \dots$, M is a number of mini-resonators, $\delta_{in} \cong M\Delta$, the line width γ_b of the mini-resonators is already taken into account in the solution (7), so the limit $\text{Lim}_{\gamma_b \rightarrow 0}$ is taken in expression (9).

The use of general solutions (7) and (8) in the analytical study of the dynamics of storing and retrieval of signal fields can be significantly simplified by taking into account the spectral properties of signal fields. Here special attention should be also paid to the influence of the spectral parameters of the mini-resonators. Namely, it is well known that the comb-like nature of this spectrum can manifest itself in the appearance of multiple echo signals, which has been studied repeatedly in AFC protocols of QM (see the reviews [4, 5, 7]). In this paper, we will primarily focus on the storage stage of short signals in the considered QM scheme. During this stage, the narrow lines of the mini-resonators do not have time to manifest themselves, moreover, the spectral interval between the nearest frequencies of the mini-resonators Δ also reveals itself only after a time interval significantly exceeding the duration of the signal pulse $\tau = 2\frac{\pi}{\Delta} \gg \delta t_s$. In this case, the dynamics of the interaction of the signal pulse with the QM is influenced by the envelope of the spectrum of the resonance lines of atoms and mini-resonators.

For simplicity of the experimental implementation of the quantum memory scheme under consideration, we also assume that spectral width of signal pulses is much smaller than the inhomogeneous broadening of the atomic optical transition $\delta\omega_s \ll \Delta_{in}$. In this case

$$\frac{N_m f_m^2}{\Delta_{in,a} - i\omega} \cong \Gamma_{a,m}^0 (1 + i \frac{\omega}{\Delta_{in,a}}) = \Gamma_{a,m}^0 + i \tilde{\chi} \omega, \quad (10)$$

where $\Gamma_{a,m}^0 = \frac{N_m f_m^2}{\Delta_{in,a}}$ is the relaxation constant, which reflects the absorption rate of the m -th resonator mode by the atoms of this resonator, $\Delta_{in,a} = \Delta_{in} + \gamma_a$.

Using this approximation in $M_m(\Delta_m - \omega)$, we obtain

$$M_m(\Delta_m, \omega) \cong \frac{\chi}{\chi(\gamma_b + \Gamma_{a,m}^0) + i(\chi\Delta_m - \omega)}. \quad (11)$$

where $\chi = \frac{1}{1-\tilde{\chi}} \cong 1 + \tilde{\chi}$.

Thus, the interaction with atoms shifts the mini-resonator line ($\Delta_m \rightarrow \chi\Delta_m$), increases its linewidth ($\gamma_b \rightarrow \chi(\gamma_b + \Gamma_{a,m}^0)$) and coupling constant with a common resonator ($g_m \rightarrow \chi g_m$). Taking into account large inhomogeneous broadening ($\Delta_{in}\delta t_s \gg 1$, where δt_s is a temporal duration of a signal pulse) in Eqs.(5) and (7), we find a solution for $b_m(t)$:

$$b_m(t) \cong -ig_m^* \chi \int_{-\infty}^t dt' \exp\{-\chi(i\Delta_m + \gamma_b + \Gamma_{a,m}^0)(t - t')\} a(t'), \quad (12)$$

The large inhomogeneous broadening of the atomic transition ($\Delta_{in} \gg \delta_{in}$ where δ_{in} is a linewidth of multi-resonator system, see Fig. 2) allows using the same atomic ensembles in each mini-resonator. Assuming the atomic ensembles in each of the resonators to be identical (i.e. $\Gamma_{a,m}^0 = \Gamma_a^0$), we will have for the total attenuation constant of each mini-resonator $\Gamma_{a,m}^0 + \gamma_b \equiv \Gamma_a^0 + \gamma_b = \Gamma_\Sigma$ ($\Gamma_a^0 = \frac{N_a f_a^2}{\Delta_{in,a}}$, N_a is a number of atoms in each mini-resonator f_a is an average coupling constant).

In carrying out further calculations, we will focus on studying the temporal dynamics at times shorter than the time of automatic rephasing of mini-resonators $\tau = \frac{2\pi}{\Delta}$. On such short time intervals we can describe the frequencies of mini-resonators by moving from a discrete to a continuous distribution function $G_r(\Delta_m/\delta_{in})$:

$$\sum_m |g_m|^2 \dots \rightarrow Mg^2 \int d\Delta_m G_r\left(\frac{\Delta_m}{\delta_{in}}\right) \dots \quad (13)$$

There are two interesting options for describing the frequency distribution of mini-resonators. In the first case, which takes place in a real experiment, we have mini-resonators that form a comb of natural frequencies with a distance Δ between the nearest frequencies. The frequency distribution envelope has a rectangular shape with a total spectrum width δ_{in} (i.e. $G_{r,1}(\Delta_m/\delta_{in}) = \frac{1}{\delta_{in}}$ for $|\Delta_m| \leq \frac{\delta_{in}}{2}$ and $G_{r,1}(\dots) = 0$ for $|\Delta_m| > \frac{\delta_{in}}{2}$). When the spectral width of the signal spectrum $\delta\omega_s$ δ_{in} is less than the spectral width of the mini-resonators, the description of the frequencies of the mini-resonators can be also simplified by using the Lorentzian form ($G_{r,2}(\Delta_m/\delta_{in}) = \frac{\delta_{in}}{\pi(\delta_{in}^2 + \Delta_m^2)}$). In a further analysis, we will compare the results of these two descriptions.

Taking into account the continuous distribution of the frequencies of the mini-resonators in the Eq. (8), after carrying out calculations we obtain

$$\tilde{a}(\omega) = T_{cw}(\omega) \tilde{A}_{in}(\omega) = \frac{\sqrt{\kappa} \tilde{A}_{in}(\omega)}{\left(\frac{1}{2}\kappa + \gamma_c + \frac{Mg^2}{\delta_{in}\mathcal{F}_{1,2}(\chi\delta_{in}, \chi\Gamma_\Sigma, \omega)} - i\omega\right)}, \quad (14)$$

where $\mathcal{F}_1(\dots)$ and $\mathcal{F}_2(\dots)$ correspond to two variants of resonator frequency distribution:

$$\mathcal{F}_1(\dots) = \frac{1}{(\pi - [\phi_{(+)}(\dots) + \phi_{(-)}(\dots)] + i \ln[\mathcal{B}(\dots)])}, \quad (15)$$

$$\mathcal{F}_2(\dots) = \left(1 + \frac{\chi\Gamma_\Sigma - i\omega}{\chi\delta_{in}}\right), \quad (16)$$

where $\mathcal{B}(\dots) = \sqrt{\frac{(\frac{1}{2}\chi\delta_{in} + \omega)^2 + (\chi\Gamma_\Sigma)^2}{(\frac{1}{2}\chi\delta_{in} - \omega)^2 + (\chi\Gamma_\Sigma)^2}}$ and $\phi_{(\pm)}(\dots) = \arctan\left(\frac{2\chi\Gamma_\Sigma}{\chi\delta_{in} \pm 2\omega}\right)$ herewith $\phi_{(\pm)}(\dots) < \pi/2$ if $\omega = 0$.

The analytical solution in equation (16) can be very convenient for analyzing the properties of QM in the case of using narrow-band signal fields. It is noteworthy that the analytical solution (15) was obtained with a realistic system of mini-resonators. Below we will focus only on some interesting situations.

In the limit of narrow band signal pulse $\delta\omega_s \ll \delta_{in}$ in Eq.(15), we get for $\mathcal{F}_1(\chi\delta_{in}, \chi\Gamma_\Sigma, \omega)$:

$$\mathcal{F}_1(\dots) \cong \frac{1}{\left(\pi - 2 \arctan\left(\frac{2\Gamma_\Sigma}{\delta_{in}}\right) + i \frac{4\delta_{in}\frac{\omega}{\chi}}{\delta_{in}^2 + 4\Gamma_\Sigma^2 + 4(\frac{\omega}{\chi})^2}\right)} \Big|_{\Gamma_\Sigma \ll \delta_{in}} \approx \frac{1}{\pi} \left(1 + 4 \frac{\chi\Gamma_\Sigma - i\omega}{\pi\chi\delta_{in}}\right), \quad (17)$$

which is completely analogous to the function \mathcal{F}_2 with Lorentzian shape in Eq. (16) for arbitrary spectral width of a signal pulse if $\Gamma_\Sigma \ll \delta_{in}$. From the Eqs. (15) - (17) it is evident that when interacting with a common resonator, a system of mini-resonators loaded with atomic ensembles acquires a larger spectral widths $\delta_{in} + \frac{4}{\pi}\Gamma_\Sigma$ and $\delta_{in} + \Gamma_\Sigma$ in the two cases of frequency distributions of mini-resonators.

The Eq. (14) is the first main result obtained, which only takes into account the assumption of a large inhomogeneous broadening of the atomic transition ($\Delta_{in} \gg \delta t_s^{-1}, \delta_{in}$). Below, using the solution (14) we analyze the QM dynamics and determine the physical parameters providing high efficiency and broadband storage of a signal light pulse. Applying the relation connecting the input and output fields with the field of a common resonator [34] $A_{in}(t) + A_{out}(t) = \sqrt{\kappa}a(t)$, we get

$$\begin{aligned} \tilde{A}_{out}(\omega) = & U(\omega) \tilde{A}_{in}(\omega) = \\ = & \left(\frac{1}{2} \kappa - \gamma_c - \frac{Mg^2}{\delta_{in} \mathcal{F}_{1,2}(\chi \delta_{in}, \chi \Gamma_\Sigma, \omega)} + i\omega \right) \tilde{A}_{in}(\omega) \\ = & \left(\frac{1}{2} \kappa + \gamma_c + \frac{Mg^2}{\delta_{in} \mathcal{F}_{1,2}(\chi \delta_{in}, \chi \Gamma_\Sigma, \omega)} - i\omega \right) \tilde{A}_{in}(\omega). \end{aligned} \quad (18)$$

By taking the carrier frequency of the signal pulse equal to zero $\omega = 0$ in the equation, we obtain the impedance matching condition:

$$\kappa = 2\gamma_c + \frac{2Mg^2}{\delta_{in} \mathcal{F}_{1,2}(\chi \delta_{in}, \chi \Gamma_\Sigma, 0)}, \quad (19)$$

which provides close to 100% transfer of an input signal to the system of resonators + atoms. Comparing (19) with the solution for multiresonator QM without using atomic ensembles [22], we find that the interaction of mini-resonators with atomic ensembles is manifested in (19) by increasing the total spectral width of the frequency comb of mini-resonators ($\delta_{in} \rightarrow \delta_{in} \mathcal{F}_{1,2}(\chi \delta_{in}, \chi \Gamma_\Sigma, 0) > \delta_{in}$) (where $\mathcal{F}_{1,2}(\chi \delta_{in}, \Gamma_\Sigma, 0) > 1$ and it is a growing function of Γ_Σ see Eqs.(17), (16)). Thus, the interaction with the atomic ensembles reduces the coupling constant κ required to satisfy the impedance matching condition. This effect increases with ratio $\frac{\Gamma_\Sigma}{\delta_{in}}$.

Let's take a closer look at it for the first (rectangular) variant of the mini-resonator frequencies. Here we get from Eq. (19):

$$\kappa = 2\gamma_c + 2\pi \frac{g^2}{\Delta} \left(1 - \frac{2}{\pi} \arctan \left(\frac{2\Gamma_\Sigma}{\delta_{in}} \right) \right). \quad (20)$$

This solution is valid for arbitrary parameters included in it and shows that enhancing the interaction of mini-resonators with atomic ensembles reduces the coupling constant of the common resonator with the waveguides κ , which is necessary for impedance matching condition. Two limiting cases are interesting.

1) The case of weak interaction between atomic ensemble with mini-resonator ($\frac{\Gamma_\Sigma}{\chi \delta_{in}} < 1$):

$$\kappa \cong 2\gamma_c + 2\pi \frac{g^2}{\Delta} \left(1 - \frac{4\Gamma_\Sigma}{\pi \delta_{in}} \right), \quad (21)$$

which transfers to impedance matching condition of empty mini-resonators [22] for $\frac{4\Gamma_\Sigma}{\pi \delta_{in}} \ll 1$.

2) Strong interaction of atoms with mini-resonator ($\frac{2\Gamma_\Sigma}{\delta_{in}} \gg 1 \rightarrow \arctan[\frac{2\Gamma_\Sigma}{\delta_{in}}] \approx \frac{\pi}{2} - \frac{\delta_{in}}{2\Gamma_\Sigma}$):

$$\kappa \cong 2\gamma_c + 2\pi \frac{g^2}{\Delta} \frac{\delta_{in}}{\pi \Gamma_\Sigma} = 2\gamma_c + \frac{2Mg^2}{\Gamma_\Sigma}, \quad (22)$$

where $\frac{2Mg^2}{\Gamma_\Sigma} \ll \frac{2\pi g^2}{\Delta}$, which describes the interaction of a common resonator with identical M mini resonators

having a spectral width Γ_Σ an increase in which leads to a narrowing of the working spectral range. For the effective implementation of broadband QM, it is necessary to limit the increase of Γ_Σ in order to preserve the condition $\frac{Mg^2}{\Gamma_\Sigma} \gg \gamma_c$.

3) mini-resonators with Lorentzian frequency distribution. Using Eqs. (16) and (19), we get the following impedance matching condition:

$$\kappa = 2\gamma_c + \frac{2Mg^2}{(\delta_{in} + \Gamma_\Sigma)}. \quad (23)$$

Thus, the well-known impedance matching condition ($\kappa = 2\gamma_c + \frac{2Mg^2}{\delta_{in}}$) is obtained only if $\delta_{in} \gg \Gamma_\Sigma$.

Below we analyze in detail the conditions for implementing highly efficient storage of the signal pulse, and the influence of the interaction of mini-resonators with atoms on this process.

B. Spectral impedance matching condition

Returning again to the solution that writes the spectrum of reflected radiation (18), we add spectral impedance matching condition

$$\frac{4Mg^2}{(\chi \delta_{in})^2 + 4(\chi \Gamma_\Sigma)^2} = 1. \quad (24)$$

If it is satisfied, the transfer function $U(\omega)$ (and $T(\omega)$ in Eqs.(14)) will only depend quadratically on the frequency offset ω leading to the broadening of the working spectral width of the QM similar to the QM for atoms in a single resonator [17]. Taking spectral matching into account in Eq. (19) leads to the following expression for the basic impedance matching condition:

$$\begin{aligned} \frac{\kappa}{2} = & \gamma_c + \chi \frac{\delta_{in}^2 + 4\Gamma_\Sigma^2}{4\delta_{in}} \left(\pi - 2 \arctan \left(\frac{2\Gamma_\Sigma}{\delta_{in}} \right) \right) \Big|_{\Gamma_\Sigma \ll \delta_{in}} \\ \cong & \gamma_c + \frac{\pi}{4} \chi \delta_{in} \left(1 - \frac{4\Gamma_\Sigma}{\pi \delta_{in}} \right). \end{aligned} \quad (25)$$

where the case of the predominance of inhomogeneous broadening over the constant of interaction of an ensemble of atoms with mini-resonators is also noted (and $\chi \delta_{in} \gg \frac{4}{\pi} \gamma_c$ is needed). The graphs in Fig. 3 show the behavior of the spectral reflection function $|U(\omega)|^2$ (see Eq. (18)) for different parameters of the system under study. Comparison of the graphs (black solid and red dashed-dotted lines) in Fig. 3 demonstrates the influence of the interaction of atoms with mini-resonators on the impedance matching conditions (see spectral range near $\omega = 0$). Blue dashed line in Fig. 3 demonstrates that taking into account the spectral matching condition (24) greatly expands the spectral range of QM in comparison with the other two graphs.

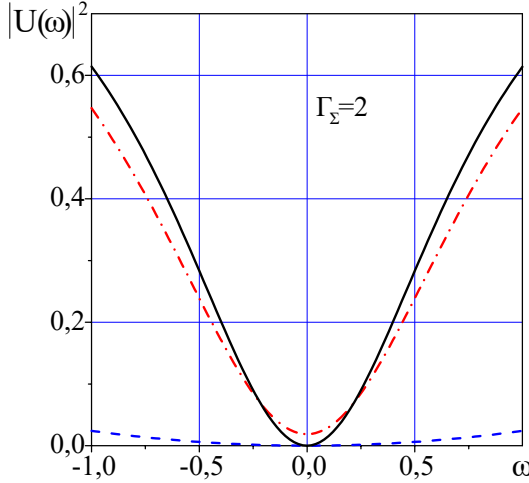


Рис. 3. Spectral reflection function $|U(\omega)|^2$: the red dashed-dotted line corresponds to the reflection under the impedance matching condition (20), neglecting in this condition the interaction of mini-resonators with atoms; black solid line - taking into account in the condition (20) the interaction of mini-resonators with atomic ensembles where $\kappa = 1$, $\delta_{in} = 10$, $\Gamma_\Sigma = 2$; blue dashed line - taking into account two impedance matching conditions (20) and (24) where $\Gamma_\Sigma = 2$, $\delta_{in} = 10$, $\kappa = 15.51$.

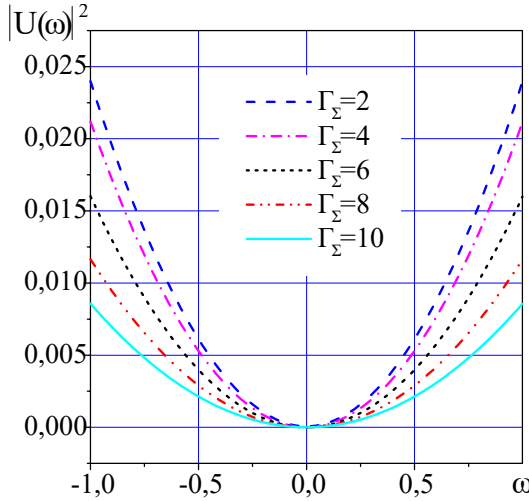


Рис. 4. Spectral reflection function $|U(\omega)|^2$ with two impedance matching conditions (20) and (24): $\delta_{in} = 10$, $\Gamma_\Sigma = 2, 4, 6, 8, 10$ at ($\kappa = 23.17$ for $\Gamma_\Sigma = 10$).

Fig. 4 shows graphs of the spectral behavior of reflection for different strengths of interaction of mini-resonators with atomic ensembles. The graphs show that an increasing the interaction constant Γ_Σ of mini-resonators with atoms can lead to a spectral broadening of the effective light storage (when the interaction constant Γ_Σ increases from $0.2\delta_{in}$ to δ_{in}). At the same time, the storage efficiency reaches 99 % within the spectral range $0.2\delta_{in}$ (see curves with $\Gamma_\Sigma=8$ and 10, where $\kappa = 23.17$ with $\delta_{in} = 10$).

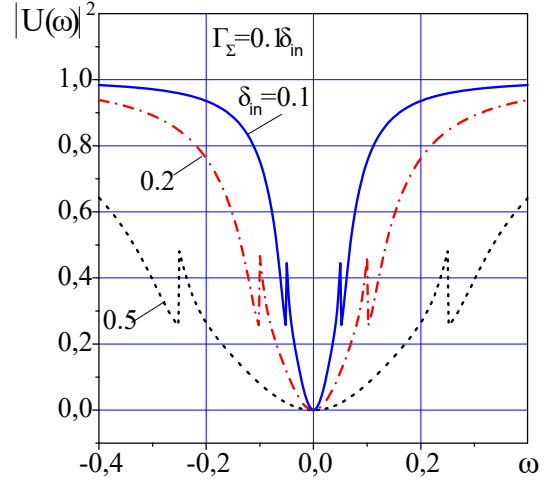


Рис. 5. Spectral reflection function $|U(\omega)|^2$ with two impedance matching conditions (20) and (24): $\Gamma_\Sigma = 0.1\delta_{in}$, linewidth $\delta_{in} = 0.1, 0.2, 0.5$ (the constant $\kappa = 0.766$ with a spectrum width $\delta_{in} = 0.5$).

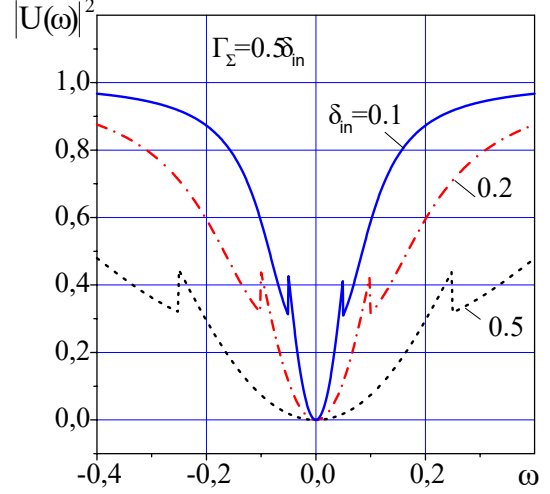


Рис. 6. Spectral reflection function $|U(\omega)|^2$ with two impedance matching conditions (20) and (24): $\Gamma_\Sigma = 0.5\delta_{in}$, linewidth $\delta_{in} = 0.1, 0.2, 0.5$ ($\kappa = 0.785$ with $\delta_{in} = 0.5$).

Figures 5, 6 and 7 show the behavior of the spectral reflection function $|U(\omega)|^2$ for different interaction constants $\Gamma_\Sigma = 0.1\delta_{in}, 0.5\delta_{in}, 1.0\delta_{in}$ and spectral widths $\delta_{in} = 0.1, 0.2, 0.5$ of the mini-resonators under impedance matching conditions (20) and (24). Figures 5 and 6 show how the reflection changes (decreases) dramatically at the spectrum boundary of the mini-resonator system. Note that within the entire spectral range there are resonant atoms. Of interest is the presence of some weakening of the reflection at a small detuning beyond the spectrum boundaries of the mini-resonators, which is apparently explained by the manifestation of strong frequency dispersion. The general tendency to weaken the reflection with an increase in the frequency detuning from the center of the line indicates a weakening of

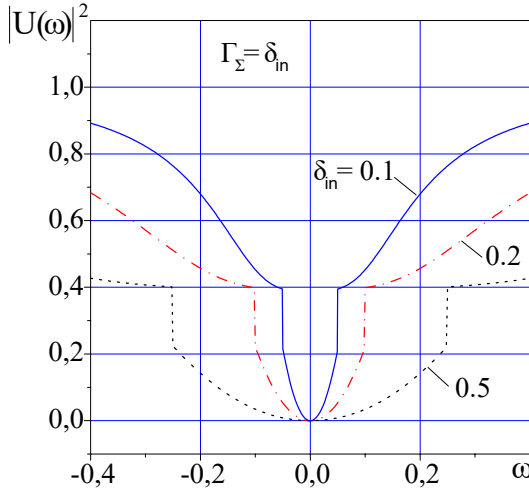


Рис. 7. Spectral reflection function $|U(\omega)|^2$ with two impedance matching conditions (20) and (24): $\Gamma_\Sigma = \delta_{in}$, linewidth $\delta_{in} = 0.1, 0.2, 0.5$ ($\kappa = 1.159$ with $\delta_{in} = 0.5$).

the interaction of the signal pulse with atoms whose spectrum is beyond the spectrum of the mini-resonators and a departure from the impedance matching condition.

As can be seen from Fig. 7, an increase in interaction with atoms Γ_Σ leads to a weakening of the reflection of the signal within the spectrum of mini-resonators, which is manifested in a deepening of the minimum of the function $|U(\omega)|^2$. It is also noteworthy that, in contrast to the weak interaction of atoms with mini-resonators, there is no longer a jump in the decrease in signal reflection when going beyond the spectrum of mini-resonators. The presented graphs of the Figs. 4-7 allow us to conclude that the strengthening of the interaction of mini-resonators with atomic ensembles leads to an improvement in the spectral properties of QM. It is also seen that the rectangular nature of the frequency distribution of mini-resonators $G_{r,1}(\Delta_m/\delta_{in})$ leads to a quadratic dependence on the behavior of the spectral efficiency. In this connection, an even greater increase in the working spectral width of QM requires the introduction of a frequency dependence of the interaction constant (g_m) of mini-resonators with a common resonator, which be a subject of further studies.

Until now we have been interested in the joint manifestations of mini-resonators with atoms in the absorption of a signal pulse by a QM cell. However, the implementation of long-lived QM involves timely and highly efficient transfer of a signal pulse to atomic ensembles from mini-resonators. To clarify this process it is necessary to consider its spectral and temporal behavior in more detail, taking into account that the system of mini-resonators is phased over time $\tau = 2\pi/\Delta \gg \delta t_s \sim \delta\omega_s^{-1}$, which can change its interaction with the common resonator.

C. Dynamics of mini-resonators and atoms

Important information about the properties of the signal pulse absorption can be obtained by sequentially examining the behavior of atomic coherence and field amplitude in m -th mini-resonator. By using Eq.(14) and (12) we get the spectral response $\tilde{b}_m(\omega)$ of the m -th resonator mode to the signal radiation:

$$\tilde{b}_m(\omega) = -ig_m^* \frac{\chi T_{cw}(\omega)}{(\chi\Gamma_\Sigma + i(\chi\Delta_m - \omega))} \tilde{A}_{in}(\omega). \quad (26)$$

Taking into account the flat vertex in the spectral dependence of the $T(\omega)$ function, Eq. (36) describes the Lorentzian shapes of excitation of the m -th mode with a slightly shifted eigen frequency ($\Delta_m \rightarrow \chi\Delta_m$) and considerably increased spectral width ($\gamma_b \rightarrow \gamma_b + \Gamma_a^0 \gg \gamma_b$) due to the interaction with m -th atomic ensemble.

Going to time domain, we consider a fairly short signal pulse satisfying the condition $(\gamma_b + \Gamma_a^0)\delta t_s \ll 1$, but it has a sufficiently narrow spectral width according to Eq.(14) and taking into account (25) (see Figs.4-7), we get field mode in the common resonator for times $t < (\Gamma_a^0)^{-1}$:

$$a(t) \cong \frac{A_{in}(t)}{\sqrt{\kappa}}. \quad (27)$$

The solution (27) describes the fast transfer of a signal pulse into a system of mini-resonators from the common resonator. Having the solutions Eqs. (12) and (27), we obtain for the time evolution of the m -th field mode in this case:

$$b_m(t > \delta t_s) \approx -i\sqrt{2\pi} \frac{g_m^* \chi}{\sqrt{\kappa}} \tilde{A}_{in}(\chi\Delta_m) \cdot \exp\{-i(\chi\Delta_m + \chi\gamma_b + \chi\Gamma_a^0)t\}, \quad (28)$$

which shows that m -th mini-resonator captures the spectral component $\chi\Delta_m$ of the signal field practically during the duration of the signal pulse δt_s . We can also estimate the behavior of the degree of excitation $P_M(t)$ of the mini-resonator system assuming a sufficiently large spectral width of the mini-resonator $\delta_{in} \gg \delta\omega_s$. In this case, without affecting the result of the calculations, we used the Lorentzian distribution of mini-resonator frequencies $G_r(\Delta_m/\delta_{in}) = G_{r,L}(\Delta_m/\delta_{in}) = \frac{\delta_{in}}{\pi(\delta_{in}^2 + \Delta_m^2)}$. Using (28) we get:

$$\begin{aligned} P_M(t) &= \sum_m^M |b_m(t)|^2 \\ &\approx 2\pi \frac{Mg^2\chi^2}{\kappa} \exp\{-2\chi(\gamma_b + \Gamma_a^0)t\} \cdot \\ &\quad \int \Delta_m \frac{\delta_{in}}{\pi(\delta_{in}^2 + \Delta_m^2)} |\tilde{A}_{in}(\chi\Delta_m)|_{\delta_{in} \gg \delta\omega_s}^2 \\ &\approx 2 \frac{Mg^2\chi}{\kappa\delta_{in}} \exp\{-2\chi(\gamma_b + \Gamma_a^0)t\} W_{in}, \end{aligned} \quad (29)$$

where $W_{in} = \int_{-\infty}^{\infty} dt |A_{in}(t)|^2$ is a number of photons in an input light pulse. Considering also $\delta_{in} \gg \Gamma_a^0$, $\chi \approx 1$ with impedance matching condition (23) in Eq. (29), we get exponential energy loss from the mini-resonator system:

$$P_M(t) \approx W_{in} \exp\{-2\chi(\gamma_b + \Gamma_a^0)t\}. \quad (30)$$

The solution (30) describes the limit case of a very short signal pulse and a very large spectral width of the spectrum of the mini-resonators ($\delta_{in} \gg \Gamma_a^0$). The solution (30), based on the assumption of very fast signal transmission from the common resonator to the mini-resonator system allows us to understand the rate of signal pulse energy transmission from the mini-resonator system to the atomic ensembles. However, it does not take into account the influence of interaction with atoms on the transfer of the signal pulse to the mini-resonator system from the common resonator. We can obtain more detailed information about the dynamics of the behavior of the mini-resonator system using the Eq. (12). Carrying out similar calculations under the assumption that $\delta_{in} \gg \delta\omega_s$ and $\delta_{in} - \Gamma_\Sigma \gg \delta\omega_s$ ($\delta_{in} > \Gamma_\Sigma$):

$$P_M(t) = \sum_m^M |b_m(t)|^2 \cong \frac{2Mg^2}{\kappa} \frac{\delta_{in}}{(\delta_{in}^2 - \Gamma_\Sigma^2)} \cdot \{\chi \int_{-\infty}^t dt' |A_{in}(t')|^2 e^{-2\chi\Gamma_\Sigma(t-t')} - \frac{|A_{in}(t)|^2}{2\delta_{in}}\}. \quad (31)$$

In the limit $\delta_{in} \gg \Gamma_\Sigma$ and $\delta\omega_s \gg \Gamma_\Sigma$, the solution (31) comes down to the solution (30). As can be seen from the solution (31), when deviating from these conditions, the excitation dynamics of the mini-resonator changes noticeably at the stage of interaction with the input signal pulse. After the end of the impulse, the second term in Eq. (31) disappears and the solution takes the form:

$$P_M(t) \cong \frac{2Mg^2\chi}{\kappa} \frac{\delta_{in}}{(\delta_{in}^2 - \Gamma_\Sigma^2)} e^{-2\chi\Gamma_\Sigma t} \int_{-\infty}^{t > \delta t_s} dt' |A_{in}(t')|^2 e^{2\chi\Gamma_\Sigma t'}. \quad (32)$$

Thus after the signal pulse has entered the mini-resonators and its duration is shorter than Γ_Σ^{-1} , we see exponential decay of energy captured in all the mini-resonators: All the trapped signal energy is transferred into the atomic ensemble with a rate $\chi\Gamma_\Sigma$ provided that $\Gamma_a^0 \gg \gamma_b$, which is necessary to minimize irreversible signal pulse losses in mini-resonators. The main part of the light energy will be transferred with high efficiency to atoms during time interval T satisfying the condition $\Gamma_a^0 T \geq 3$. At the same time, if 5 mini-resonators are used, no more than 1.2 % energy remains in them at

time $t = T$. However, this process can continue as long as the mini-resonators are out of phase with respect to each other, i.e. if $T < \tau = \frac{2\pi}{\Delta}$, for example at $T = \tau/2 > 3(\Gamma_a^0)^{-1}$. Accordingly, we obtain the following more strong condition

$$\Gamma_a^0 = \frac{N_a f_a^2}{\Delta_{in,a}} \geq 6/\tau = \frac{3\Delta}{\pi}, \quad (33)$$

providing highly efficient transfer of signal light to atomic ensembles if $N_a \geq \frac{3\Delta}{\pi} \cdot \frac{\Delta_{in,a}}{f_a^2}$. At the same time, it is necessary to note here the conditions for the atomic coherence time $T_2 = \gamma_a^{-1}$ and the eigen linewidth γ_b of the mini-resonators: $T_2 \gg 2\pi/\Delta$ and $2\pi\gamma_b/\Delta \ll 1$. The latter condition, together with the condition for a coupling constant between resonators and atomic ensembles Γ_a^0 , imposes basic requirements both for a high Q-factor of mini-resonators ($Q \gg \frac{\pi\omega_c}{\Delta}$, where ω_c is a frequency of mini-resonator). Having the relations Eqs.(19), (20) and Eq. (33), we can estimate how much easier the requirements are for using atomic ensembles for multiresonator QM in relation to single-resonator QM. The implementation of QM on an atomic ensemble in one resonator implies the fulfillment of the matching condition $\frac{N_s f_s^2}{\Delta_{in,a}} = \kappa/2$ [17, 26] (f_s is a coupling constant of atoms with a single resonator) and comparing it with the condition Eq.(33). Comparing the number of atoms (N_s and N_a) in these two versions of QM implementation, we find the number of atoms N_a required for use in the one mini-resonator of the QM under study

$$N_a \approx \frac{6\Delta}{\pi\kappa} \left| \frac{f_s}{f_a} \right|^2 N_s, \quad (34)$$

which is at least in $\frac{\pi\kappa}{6\Delta} \gg 1$ times less than N_s . This quantitative estimate, which specifies the observation made earlier in [29]. Interestingly, if we assume that the total number of mini-resonators M fills a spectral range equal to a κ ($M\Delta \cong \kappa$), then the total number of atoms in all resonators will equal the number of atoms in a single-resonator quantum memory. But in mini-resonators, the coupling constant with atoms f_a can be significantly stronger than the constant f_s in a single larger resonator, which will lead to a significant decrease in the total number of atoms N_a .

It is also important to keep in mind that increasing the coupling constant of the interaction of atomic ensembles with the mini-resonator $\Gamma_a^0 = \frac{N_a f_a^2}{\Delta_{in}}$ can lead to too large a narrowing of the working spectral range (see Eqs. (19)-(25)). The implementation of the impedance matching condition is significantly simplified by the fact that it depends to a greater extent on the parameters of the interaction of the mini-resonators with the main resonator. It becomes easy to fulfill this condition when the coupling constants between the resonators $g_m \equiv g$ can be chosen to be large enough.

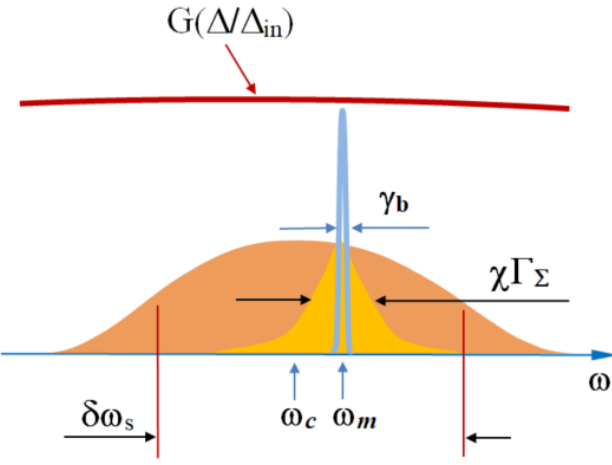


Рис. 8. Spectrum of excited atoms in m -th mini-resonator which has Lorentzian shape with spectral width $\chi\Gamma_\Sigma \geq \frac{3\Delta}{\pi}$, γ_b and $\delta\omega_s$ are the spectral widths of the eigenmode of the mini-resonator and the signal pulse.

The next important issue is to clarify the parameters of the exited atomic state resulting from the storage of a signal pulse. Using Eqs.(4) and (12), we get for $t \geq T$:

$$S_{j,m}(t) = -i\sqrt{2\pi}f_{j,m}^*e^{-(i\delta_{j,m}+\frac{1}{2T_1})t+i\delta\phi_{j,m}(t)}\tilde{b}_m(\delta_{j,m}), \quad (35)$$

$$\tilde{b}_m(\omega) = -ig_m^*\frac{\chi T_{cw}(\omega)}{(\chi\Gamma_\Sigma + i(\chi\Delta_m - \omega))}\tilde{A}_{in}(\omega). \quad (36)$$

where we have concretized the nature of the decay of atomic coherence, highlighting the appearance of a random phase shift $\delta\phi_{j,m}(t)$ and the manifestation of the transition of the atom to other energy states determined by the time T_1 of longitudinal (energy) relaxation. Probability of j, m -th atom to be in excited state will be:

$$|S_{j,m}(t)|^2 = e^{-\frac{t}{T_1}}|T_{a,m}(\chi\Delta_m - \delta_{j,m})|^2 \cdot |T_{c,w}(\delta_{j,m})|^2|\tilde{A}_{in}(\delta_{j,m})|^2, \quad (37)$$

where

$$|T_{a,m}(\chi\Delta_m - \delta_{j,m})|^2 = \frac{2\pi\chi^2|fg|^2}{(\chi\Gamma_\Sigma)^2 + (\chi\Delta_m - \delta_{j,m})^2}. \quad (38)$$

In the calculations above, we assumed $f_{j,m} = f_a$, $g_m = g$ (see also Eq.(14)).

In the physical sense, the transfer function $|T_{c,w}(\delta_{j,m})|^2$ describes the probability of transferring the frequency mode $\omega = \delta_{j,m}$ of a signal photon from the waveguide to the common resonator. When both impedance matching

conditions of agreement are met $|T_{c,w}(\delta_{j,m})|^2 \cong \frac{1}{\kappa}$. The function $|T_{a,m}(\chi\Delta_m - \delta_{j,m})|^2$ describes the probability of transferring this spectral mode from the common resonator to the j -th atom of the m -th mini-resonator. Thus, as can be seen in Fig. 8, atoms are excited in the m mini-resonator near the natural frequency of this mini-resonator $\chi\Delta_m$ inside the spectral range $\chi\Gamma_\Sigma$ described by the Lorentzian form of (38). Due to the interaction with the atomic ensemble, the coefficient χ slightly shifts the eigen frequency of the m -th mini-resonator. The spectral width of excited atoms is close to the spectral interval between the nearest modes of mini-resonators $\chi\Gamma_\Sigma \geq \frac{3\Delta}{\pi} \approx \Delta \gg \gamma_b$, significantly exceeding the eigen spectral width of the mini-resonator mode. Thus, the atoms excited in all the mini-resonators completely overlap the spectrum of the signal pulse.

The expression (37) reflects an important property of recording a signal pulse in a system of atoms in a mini-resonator. Namely, no matter how small the intrinsic spectral width of the resonator γ_b , the signal is stored in a wider spectrum of atoms $\chi\Gamma_a^0 \gg \gamma_b$, which is determined by the collective interaction of atoms (the spectral density of the atomic transitions and average coupling constant) with the field mode of m -th mini-resonator. An important conclusion follows from this: if, for example, between the common resonator and the mini-resonators we even place another, narrower-band resonators, then, its use will not allow us to narrow the spectral width of the signal pulse storage in the mini-resonators, which will still be determined by a constant $\chi\Gamma_\Sigma \gg \gamma_b$.

By assuming a sufficiently narrow spectrum of a signal pulse $\delta\omega_s < \kappa/3$ and $\Gamma_\Sigma \gg \gamma_b$, we evaluate the transfer of this pulse to the all atomic ensembles ($t > \Gamma_\Sigma^{-1}$) by using Eq. (37):

$$P_a(t) = \sum_m^M \sum_j^{N_m} |S_{j,m}(t)|^2 = \frac{2\pi MN}{\kappa} e^{-\frac{t}{T_1}} \int d\Delta_m \frac{\delta_{in}}{\pi(\delta_{in}^2 + \Delta_m^2)} \int d\delta_{j,m} \frac{\Delta_{in}}{\pi(\Delta_{in}^2 + \delta_{j,m}^2)} \frac{|fag|^2}{\Gamma_\Sigma^2 + (\Delta_m - \frac{\delta_{j,m}}{\chi})^2} |\tilde{A}_{in}(\delta_{j,m})|^2. \quad (39)$$

Assuming a large inhomogeneous broadening of the atomic atomic transition, we have $\frac{\Delta_{in}}{(\Delta_{in}^2 + \delta_{j,m}^2)} \cong \frac{1}{\Delta_{in}}$. Next we calculate the integral $\int d\Delta_m \dots$ when $\delta_{in} \pm \Gamma_\Sigma \gg \delta\omega_s$ that leads to

$$P_a(t) \cong e^{-\frac{t}{T_1}} \frac{2M|g|^2}{\kappa(\delta_{in} + \Gamma_\Sigma)} \frac{N|f_a|^2}{\Delta_{in}\Gamma_\Sigma} \int d\omega |\tilde{A}_{in}(\omega)|^2 = e^{-\frac{t}{T_1}} E_1 E_2 W_{in}. \quad (40)$$

where $E_1 = \frac{(\kappa - 2\gamma_c)}{\kappa}$, $E_2 = \frac{\Gamma_a^0}{\Gamma_a^0 + \gamma_b}$ and we used impedance matching condition (23), $\Gamma_\Sigma = \Gamma_a^0 + \gamma_b$ and $\Delta_{in} \gg \gamma_a$

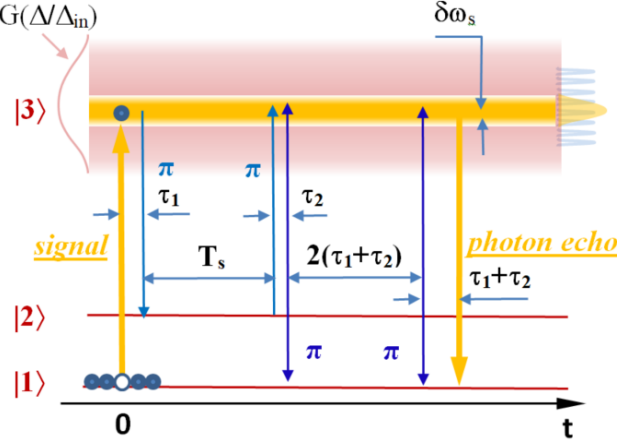


Рис. 9. A time sequence of a QM protocol with long-term storage of a signal pulse on an atomic coherence of the transition $|1\rangle \leftrightarrow |2\rangle$. The optical transition $|1\rangle \leftrightarrow |3\rangle$ is inhomogeneously broadened, and the structure of the resonant (blue) lines of the mini-resonators is shown on the right. After absorption of a signal pulse, the additional two laser π pulses are applied to the adjacent auxiliary atomic transition $|2\rangle \leftrightarrow |3\rangle$ to transfer optical coherence to the long-lived transition $|1\rangle \leftrightarrow |2\rangle$ for the storage duration T_s . At the transition $|1\rangle \leftrightarrow |3\rangle$, 2 more π pulses are applied to restore the dephased atomic coherence, which then causes the emission of a photon echo after a delay time $\tau_1 + \tau_2$.

As can be seen from the solution (40), the efficiency of signal transfer to the system of atoms is determined by two factors. The first factor E_1 describes the efficiency of signal transfer to the system of mini-resonators. Its efficiency in the presence of impedance matching is limited by the losses in the common resonator (γ_c). The second factor E_2 is determined by the transfer of radiation from the mini-resonator system to atoms and its efficiency depends on the radiation losses in the mini-resonators γ_b . This consideration implies that at the loading stage, losses in the system by atoms can be neglected. The atomic losses become significant at subsequent stages of signal pulse storage. Thus the perfect transfer (40) of a signal pulse to a system of atoms occurs, as noted above, under the condition of impedance matching within given spectral range (see above Figs. 4-7, as well as with sufficiently small losses in the common ($\gamma_c \ll \kappa$) and in the mini-resonators ($\gamma_b \ll \Gamma_a^0$). The Eq. (40) also shows that the further storage of the signal pulse energy in atoms is determined by the rate of longitudinal (energy) energy relaxation. However, the retrieval of recorded information will be largely influenced by the phase relaxation of atomic coherence at the stage of information storage in the system of atoms.

This performed analysis completes the main analytical study of the storing a signal light pulse into atomic ensembles. For long-term storage of recorded information, two laser π pulses can be applied to atomic ensembles at an adjacent transition $|2\rangle \leftrightarrow |3\rangle$ to transfer

the excited optical coherence of atoms to long-lived spin sublevels $|1\rangle \leftrightarrow |2\rangle$ (see Fig.9). The subsequent retrieval of the stored signal is realized by rephasing the excite optical atomic coherence. For example, it can be realized by applying two π pulses to each atomic ensemble following the procedures [11, 35]. However, here it is also necessary to suppress the photon echo emission after the first π pulse acting at the transition $|1\rangle \leftrightarrow |3\rangle$. This can be realized by applying additional controlled dephasing of atoms, for example, using an electric or magnetic field gradients (see, for example, [36]).

After the action of the second (last) π laser pulse, the recovering (phasing) of optical atomic coherence will start the coherent interaction of atoms with the field mode in each mini-resonator. The radiation appearing in the mini-resonators will be transmitted to the common resonator, and from it the radiation will exit into the waveguide in the form of a photon echo signal. This process in its main stages reproduces in reversed time order the process of storing the signal field, studied above. The description of this process is carried out in a similar way to the above and its numerical studies [28, 29] demonstrated its time reverse order, therefore, we do not perform its detailed analysis below. At the same time, it should be noted that complete time reversibility does not occur, which is manifested in the fact that the temporal shape of the photon echo signal reproduces the temporal shape of the input signal, and not in reversed time form as is the case in the CRIB protocol of QM [36].

Based on the analysis of the stages of the signal pulse interaction, we can estimate the overall efficiency E_Σ of the considered QM protocol (by assuming using the ideal control laser π pulses):

$$E_\Sigma = E_1^2 E_2^2 e^{-8(\tau_1 + \tau_2)\gamma_a} e^{-2T_s\gamma_{(1,2)}}, \quad (41)$$

where we have two stages, each of them is characterised by the efficiency factors E_1 and E_2 , as well as by the losses determined by the decay of atomic coherence on the transitions $|1\rangle \leftrightarrow |3\rangle$ during time interval $4(\tau_1 + \tau_2)$ and on the transition $|1\rangle \leftrightarrow |2\rangle$ during storage time T_s ($\gamma_{(1,2)}$ is a decay constant of the atomic coherence on this transition), τ_1 and τ_2 are the time intervals between signal and laser pulses (see Fig.9).

III. DISCUSSION AND CONCLUSION

A theory of QM on atomic ensembles in a multi-resonance scheme, including a common resonator and several mini-resonators containing atoms, has been developed. The analytical results obtained on its basis allowed to establish a physical picture of the process of a signal pulse storage on a system of atomic ensembles. Analytical relations determining the conditions for the effective implementation of the considered QM were obtained. The spectral properties of the QM scheme under consideration were studied in detail. It has been

established that effective quantum storage should be accompanied by the excitation of atomic coherence in each of the mini-resonators in a sufficiently large spectral range, which is determined by the collective interaction of atoms with the mini-resonator mode. This spectral range is close to the frequency interval between the frequencies of the nearest mini-resonators, exceeding the spectral width of the eigenmode of the mini-resonators.

The obtained analytical relation allows us to determine the optimal physical parameters of the considered QM, providing high efficiency within maximum spectrum width for various parameters of the atomic system interacting with mini-resonators. In this case, a spectral matching condition has been found, the fulfillment of which plays a major role in increasing the working spectral width of quantum memory. It is also shown that the enhancement of the interaction of atoms with mini-resonators strongly affects the impedance matching condition and it is found that the interaction enhancement can also lead to a significant broadening of the working spectral range of the memory.

The proposed multiresonator QM scheme can provide a significant reduction in the number of atoms required for use in mini-resonators, which opens up the possibility of weakening the decoherent effects in the system of atoms. This effect will be significantly enhanced when using small-sized mini-resonators, which is possible for whispering gallery modes in ring resonators [28, 37–39], as well as for nano-photonic resonators [40, 41]. The latter have demonstrated a significant enhancement of the Purcell effect, which makes them especially promising for the implementation of the considered QM scheme,

taking into account that nano photonic optical resonators can be easily combined into a common multiresonator scheme on a single integrated platform.

Fundamentally new possibilities in the control of optical QM appear due to the creation of a long-lived macroscopic coherence in it [42]. The implementation of such a QM in a multiresonator scheme is of particular interest, especially for the efficient quantum conversion of the photon frequency. Among potentially interesting atomic ensembles, we note rare earth ions in crystals [36, 43, 44]. By choosing one or another rare earth ion, it is possible to obtain various resonant frequencies, including working at a wavelength of $1.5 \mu\text{m}$, used in optical commercial lines. The recently demonstrated implementation of nano photonic crystals with rare earth erbium ions [45] opens up promising prospects for the implementation of the proposed QM.

In conclusion, we note that multiresonator QM may be especially interesting for new methods of controlling the quantum state of a signal pulse based on the use of the capabilities of individual dynamic control of the fields in each mini-resonator. At the same time, new physical properties in realizing the high efficiency arise when using a small number of resonators [46]. Experimental development of such QM schemes is possible using existing optical and microwave quantum technologies.

ACKNOWLEDGMENTS

The author thanks N.S.Perminov for useful discussions. This research was supported by the Ministry of Science and Higher Education of the Russian Federation (Reg. number NIOKTR 125012300688-6).

[1] M. D. Lukin, Colloquium: Trapping and manipulating photon states in atomic ensembles, *Rev. Mod. Phys.* **75**, 457 (2003).

[2] A. I. Lvovsky, B. C. Sanders, and W. Tittel, Optical quantum memory, *Nature Photonics* **3**, 706 (2009).

[3] K. Hammerer, A. S. Sørensen, and E. S. Polzik, Quantum interface between light and atomic ensembles, *Rev. Mod. Phys.* **82**, 1041 (2010).

[4] T. Chanelière, G. Hétet, and N. Sangouard, Quantum Optical Memory Protocols in Atomic Ensembles, in *Advances In Atomic, Molecular, and Optical Physics*, Advances In Atomic, Molecular, and Optical Physics, Vol. 67, edited by E. Arimondo, L. F. DiMauro, and S. F. Yelin (Academic Press, 2018) pp. 77–150, arXiv:1801.10023.

[5] M. Guo, S. Liu, W. Sun, M. Ren, F. Wang, and M. Zhong, Rare-earth quantum memories: The experimental status quo, *Frontiers of Physics* **18**, 21303 (2023).

[6] Y. Lei, F. Kimiae Asadi, T. Zhong, A. Kuzmich, C. Simon, and M. Hosseini, Quantum optical memory for entanglement distribution, *Optica* **10**, 1511 (2023), arXiv:2304.09397.

[7] S. A. Moiseev, M. M. Minnegaliev, K. I. Gerasimov, E. S. Moiseev, A. D. Deev, and Y. Y. Balega, Optical quantum memory on atomic ensembles: physical principles, experiments and possibilities of application in a quantum repeater, *Physics-Uspekhi* 10.3367/UFNe.2024.06.039694 (2024).

[8] K. Azuma, S. E. Economou, D. Elkouss, P. Hilaire, L. Jiang, H.-K. Lo, and I. Tzitrin, Quantum repeaters: From quantum networks to the quantum internet, *Rev. Mod. Phys.* **95**, 045006 (2023), arXiv:2212.10820.

[9] J. Ye and P. Zoller, Essay: Quantum Sensing with Atomic, Molecular, and Optical Platforms for Fundamental Physics, *Phys. Rev. Lett.* **132**, 190001 (2024).

[10] M. Sabooni, Q. Li, S. Kröll, and L. Rippe, Efficient quantum memory using a weakly absorbing sample, *Phys. Rev. Lett.* **110**, 133604 (2013).

[11] M. M. Minnegaliev, K. I. Gerasimov, R. V. Urmacheev, A. M. Zheltikov, and S. A. Moiseev, Linear Stark effect in $\text{Y}_3\text{Al}_5\text{O}_{12}:\text{Tm}^{3+}$ crystal and its application in the addressable quantum memory protocol, *Phys. Rev. B* **103**, 174110 (2021).

[12] Z.-Q. Zhou, C. Liu, C.-F. Li, G.-C. Guo, D. Oblak, M. Lei, A. Faraon, M. Mazzera, and H. de Riedmatten, Photonic integrated quantum memory in rare-earth doped solids, *Laser & Photonics Reviews* **17**, 2300257

(2023).

[13] S. Duranti, S. Wengerowsky, L. Feldmann, A. Seri, B. Casabone, and H. de Riedmatten, Efficient cavity-assisted storage of photonic qubits in a solid-state quantum memory, *Opt. Express* **32**, 26884 (2024).

[14] J. S. Kollath-Bönig, L. Dellantonio, L. Giannelli, T. Schmit, G. Morigi, and A. S. Sørensen, Fast storage of photons in cavity-assisted quantum memories, *Phys. Rev. Appl.* **22**, 044038 (2024).

[15] Y.-P. Liu, Z.-W. Ou, T.-X. Zhu, M.-X. Su, C. Liu, Y.-J. Han, Z.-Q. Zhou, C.-F. Li, and G.-C. Guo, A millisecond integrated quantum memory for photonic qubits, *Science Advances* **11**, eadu5264 (2025).

[16] H.-K. Lau, H. Qiao, A. A. Clerk, and T. Zhong, Efficient in situ generation of photon-memory entanglement in a nonlinear cavity, *Phys. Rev. Lett.* **134**, 053602 (2025).

[17] S. A. Moiseev, S. N. Andrianov, and F. F. Gubaidullin, Efficient multimode quantum memory based on photon echo in an optimal qed cavity, *Phys. Rev. A* **82**, 022311 (2010), Moiseev S., Gubaidullin F., Andrianov S. arXiv: 1001.1140v1, 7 Jan. 2010.

[18] E. S. Moiseev, A. Tashchilina, S. A. Moiseev, and B. C. Sanders, Broadband quantum memory in a cavity via zero spectral dispersion, *New Journal of Physics* **23**, 063071 (2021).

[19] E. S. Moiseev and S. A. Moiseev, All-optical photon echo on a chip, *Laser Physics Letters* **14**, 015202 (2016).

[20] S. A. Moiseev, K. I. Gerasimov, R. R. Latypov, N. S. Perminov, K. V. Petrovnik, and O. N. Sherstyukov, Broadband multiresonator quantum memory-interface, *Scientific Reports* **8**, 3982 (2018).

[21] Z. Bao, Z. Wang, Y. Wu, Y. Li, C. Ma, Y. Song, H. Zhang, and L. Duan, On-Demand Storage and Retrieval of Microwave Photons Using a Superconducting Multiresonator Quantum Memory, *Physical Review Letters* **127**, 010503 (2021).

[22] A. R. Matanin, K. I. Gerasimov, E. S. Moiseev, N. S. Smirnov, A. I. Ivanov, E. I. Malevannaya, V. I. Polozov, E. V. Zikiy, A. A. Samoilov, I. A. Rodionov, and S. A. Moiseev, Toward highly efficient multimode superconducting quantum memory, *Phys. Rev. Appl.* **19**, 034011 (2023).

[23] A. R. Matanin, N. S. Smirnov, A. I. Ivanov, V. I. Polozov, D. A. Moskaleva, E. I. Malevannaya, M. V. Androshuk, M. I. Teleganov, Y. A. Agafonova, D. E. Shirokov, A. V. Andriyash, and I. A. Rodionov, Superconducting integrated random access quantum memory (2025), arXiv:2506.02570 [quant-ph].

[24] K. Lange, J. Peise, B. Lücke, I. Kruse, G. Vitagliano, I. Apellaniz, M. Kleinmann, G. Tóth, and C. Klemp, Entanglement between two spatially separated atomic modes, *Science* **360**, 416 (2018).

[25] N. Perminov, D. Y. Tarankova, and S. Moiseev, Superefficient cascade multiresonator quantum memory, *Laser Physics Letters* **15**, 125203 (2018).

[26] M. Afzelius and C. Simon, Impedance-matched cavity quantum memory, *Phys. Rev. A* **82**, 022310 (2010).

[27] Y. Li, F. Abolmaali, K. W. Allen, N. I. Limberopoulos, A. Urbas, Y. Rakovich, A. V. Maslov, and V. N. Astratov, Whispering gallery mode hybridization in photonic molecules, *Laser & Photonics Reviews* **11**, 1600278 (2017).

[28] H. An, Z. Li, and M. Hosseini, Preparation-free resonator array atomic memory for on-chip quantum storage, *APL Quantum* **2**, 026134 (2025).

[29] N. Perminov, D. Tarankova, and S. Moiseev, Superefficient cascade multiresonator quantum memory, *Laser Physics Letters* **15**, 125203 (2018).

[30] E. L. Hahn, Spin echoes, *Phys. Rev.* **80**, 580 (1950).

[31] N. A. Kurnit, I. D. Abella, and S. R. Hartmann, Observation of a photon echo, *Phys. Rev. Lett.* **13**, 567 (1964).

[32] S. Moiseev and B. Ham, Photon-echo quantum memory with efficient multipulse readings, *Physical Review A—Atomic, Molecular, and Optical Physics* **70**, 063809 (2004).

[33] H. de Riedmatten, M. Afzelius, M. U. Staudt, C. Simon, and N. Gisin, A solid-state light-matter interface at the single-photon level, *Nature* **456**, 773 (2008).

[34] D. Walls and G. Milburn, *Quantum Optics*, SpringerLink: Springer e-Books (Springer Berlin Heidelberg, 2008).

[35] V. Damon, M. Bonarota, A. Louchet-Chauvet, T. ChaneliÈre, and J.-L. Le GouËt, Revival of silenced echo and quantum memory for light, *New Journal of Physics* **13**, 093031 (2011).

[36] S. A. Moiseev, K. I. Gerasimov, M. M. Minnegaliev, E. S. Moiseev, A. D. Deev, and B. Y. Yu., Echo protocols of an optical quantum memory, *Frontiers of Physics* **20**, 23301 (2025).

[37] R. Gao, H. Zhang, F. Bo, W. Fang, Z. Hao, N. Yao, J. Lin, J. Guan, L. Deng, M. Wang, *et al.*, Broadband highly efficient nonlinear optical processes in on-chip integrated lithium niobate microdisk resonators of q-factor above 108, *New Journal of Physics* **23**, 123027 (2021).

[38] J. Nijem, A. Naiman, R. Zektzer, C. Frydendahl, N. Mazurski, and U. Levy, High-q and high finesse silicon microring resonator, *Optics Express* **32**, 7896 (2024).

[39] H.-K. Lau, H. Qiao, A. A. Clerk, and T. Zhong, Efficient in situ generation of photon-memory entanglement in a nonlinear cavity, *Physical Review Letters* **134**, 053602 (2025).

[40] T. Zhong, J. M. Kindem, J. G. Bartholomew, J. Rochman, I. Craicu, E. Miyazono, M. Bettinelli, E. Cavalli, V. Verma, S. W. Nam, *et al.*, Nanophotonic rare-earth quantum memory with optically controlled retrieval, *Science* **357**, 1392 (2017).

[41] D. M. Lukin, M. A. Gündry, and J. Vučković, Integrated quantum photonics with silicon carbide: challenges and prospects, *PRX quantum* **1**, 020102 (2020).

[42] S. A. Moiseev, K. I. Gerasimov, M. M. Minnegaliev, and E. S. Moiseev, Optical quantum memory on macroscopic coherence, *Phys. Rev. Lett.* **134**, 070803 (2025).

[43] P. Goldner, A. Ferrier, and O. Guillot-Noël, Chapter 267 - rare earth-doped crystals for quantum information processing (Elsevier, 2015) pp. 1 – 78.

[44] M. Guo, S. Liu, W. Sun, M. Ren, F. Wang, and M. Zhong, Rare-earth quantum memories: The experimental status quo, *Frontiers of Physics* **18**, 21303 (2023).

[45] Y. Yu, D. Oser, G. Da Prato, E. Urbinati, J. C. Ávila, Y. Zhang, P. Remy, S. Marzban, S. Gröblacher, and W. Tittel, Frequency tunable, cavity-enhanced single erbium quantum emitter in the telecom band, *Phys. Rev. Lett.* **131**, 170801 (2023).

[46] N. S. Perminov and S. A. Moiseev, Integrated multiresonator quantum memory, *Entropy* **25**, 10.3390/e25040623 (2023).